Available online at www.sciencedirect.com
SCIENCE DIRECT®
PERGAMON
International Journal of Heat and Mass Transfer 46 (2003) 2363–2379
International Journal of HEAT and MASS TRANSFER
www.elsevier.com/locate/ijhmt

Steady-state heat conduction in multi-layer bodies

A. Haji-Sheikh [a,*], J.V. Beck [b], D. Agonafer [c]

[a] Department of Mechanical and Aerospace Engineering, The University of Texas at Arlington, 500 West First Street, Arlington, TX 76019-0023, USA
[b] Department of Mechanical Engineering, Michigan State University, East Lansing, MI 48824-1226, USA
[c] Department of Mechanical and Aerospace Engineering, The University of Texas at Arlington, Arlington, TX 76019-0018, USA

Received 1 October 2002; received in revised form 22 November 2002

Abstract

The mathematical formulation of the steady-state temperature field in multi-dimensional and multi-layer bodies is presented. The numerical examples are for two-layer bodies and they include boundary conditions of the first, second, and third kind. This study includes tables to assist the selection of eigenfunctions and computation of the eigenvalues. The computations include the contribution of contact resistance to the temperature solution. An efficient computational scheme for calculating the eigenvalues is used. For multi-dimensional, multi-layer bodies, the eigenfunctions are real if each layer is homogeneous; they may become imaginary if layers are orthotropic.

Keywords: Steady state; Analysis; Heat conduction; Multi-dimensional; Layered materials

1. Introduction

Cooling problems related to device protection have emerged in many electronic devices. Often, analytical heat conduction solutions provide important insight and tools for designing such devices when composed of some basic elements, such as composite parallelepipeds. Moreover, exact solutions to these problems are important tools in the emerging field of verification of numerically based solutions [1,2]. For these and other related problems, the analytical solution of temperature fields in three-dimensional composite layers is important. Analytical solutions can provide accurate and rapid insight into the behavior of temperature and heat flux distributions that could be difficult to realize from the numerical solutions. In addition, a steady-state solution is a useful tool to aid in the study of the structural integrity of layered devices in electronic applications.

Spreading and constriction resistances play a major role in the cooling of electronic packages. Ignoring these phenomena can be detrimental in the design of systems because hot spots may be present due to constriction or spreading of heat flow. For example, modeling as a uniform power at the base of a heat sink, when in reality the power due to the device is on a small portion of the base surface, will result in an erroneous estimation of the junction temperature. The power distribution in many of the chips in today's technologies is far from uniform since hot spots are commonly present. In many devices, over half of the power could be located in less than one third of the device area. These hot spots not only result in the junction temperature exceeding the design specification but also significantly decrease the reliability associated with thermal stresses. Interface resistance constitutes a major portion of the "thermal budget". It is estimated that the ΔT portion of the overall resistance of a first level package can be as high as 30%.

Closed form solutions to estimate spreading and or constriction resistances have been very important in the design of devices. The most widely used analytical solution for these problems is by Kennedy [3] who derived the axisymmetric temperature distribution for a cylinder with a small circular surface area heated on one end and an isothermal condition on the other end, which is the heat sink side. Since then, a number of authors have expanded

* Corresponding author. Tel.: +1-817-272-2010; fax: +1-817-272-2952.
E-mail address: haji@mae.uta.edu (A. Haji-Sheikh).

0017-9310/03/$ - see front matter
doi:10.1016/S0017-9310(02)00542-2

Nomenclature

a, b, c, d	dimensions in Fig. 1, cm
A, B	constants, in Region 1
A_{mn}	Fourier coefficients
Bi_1	$h_1 b/k_{1y}$ in Region 1
Bi_2	$h_2(c-b)/k_{2y}$ in Region 2
Bi_b	$1/R_b$
C, D	constants, in Region 2
F	a specified function
g_i	volumetric heat source in region i, W/cm^3
i, j	indices
k_{ix}	thermal conductivity in Region i along x, W/cm K
k_{iy}	thermal conductivity in Region i along y, W/cm K
k_{iz}	thermal conductivity in Region i, along z, W/cm K
m, n, p	indices
$N_{x,m}$	norms for x-direction
$N_{y,mnp}$	norms for y-direction
$N_{z,n}$	norms for z-direction
q	heat flux, W/cm^2
q_x	x-component of heat flux vector, W/cm^2
q_y	y-component of heat flux vector, W/cm^2
q_z	z-component of heat flux vector, W/cm^2
r_i	$(k_{ix}/k_{iy})^{1/2}$
R	contact resistance, cm^2 K/W
R_b	Rk_{1y}/b
R_c	$Rk_{2y}/(c-b)$
s_i	$\sqrt{k_{iz}/k_{iy}}$
T_i	temperature in Regions i, K
T_∞	ambient temperature, K
x, y, z	coordinates, cm
X	eigenfunction in x-direction
Y	eigenfunction in y-direction
Z	eigenfunction in z-direction

Greek symbols

β_m	eigenvalue for x-direction, cm^{-1}
γ_{mnp}	eigenvalue for y-direction in Region 1, cm^{-1}
η_{mnp}	eigenvalue for y-direction in Region 2, cm^{-1}
v_n	eigenvalue for z-direction, cm^{-1}
Φ	a function in Example 1
θ	temperature function
Ψ	eigenfunction, see Eq. (A.2)

that study to include a heat transfer coefficient boundary condition on the heat sink side [4]. In addition, investigators have also studied the effect of multi-layered solids with application to printed wiring board (pwb) and the resulting heat transfer phenomena [5]. That study [5] considers a multi-layered orthotropic body with a rectangular cross-section, which mimics pwb's much better than cylindrical geometry. Boundary conditions of the first and second kind on the heated side, and a boundary condition of the third kind on the heat sink side are considered. The power distribution is very general and can include many heat flux patches thus representing distinct heated devices depicting chips or first level packages on the pwb. The effect of contact resistance between the solids is also included. The boundary condition on the sides can be that of the first and second kind, that is, temperature or heat flux. This general solution considerably enhances an engineer's ability to accurately compute the temperature distribution in a variety of electronic cooling applications. Although the emphasis of this study is on verification, the fast computation time is significant for practicing engineers, since lead time for designing products is always getting shorter.

This study complements recent work on transient conduction in multi-dimensional layered materials by Haji-Sheikh and Beck [6]. Earlier, one-dimensional orthogonal solutions in a composite medium were presented by Tittle [7] who described a generalized Sturm-Liouville procedure for composite and anisotropic domains in transient heat conduction problems. Various mathematical details are in [8,9]. For the purpose of parameter estimation, Dowding et al. [10] presented an experimental and numerical study of a two-dimensional, two-layer solution with prescribed heat flux over all surfaces. Aviles-Ramos et al. [11] use the data in [10] and report that it is necessary to retain all eigenvalues, real or imaginary, to satisfy the completeness criterion of the solution in a transient problem; details are in Ref. [6].

Computation of temperature in multi-dimensional, multi-layer bodies exhibits a few features that are not commonly observed when computing the temperature in homogeneous bodies. As stated in [6], the eigenvalues may become imaginary and, therefore, the corresponding eigenfunctions will have imaginary arguments. Also, care [6] must be exercised when computing the eigenvalues since the spacing between successive eigenvalues changes between zero and a maximum value. This work includes a procedure to target a band within which only one eigenvalue will be located as reported in [12] and a hybrid root finding scheme [12] is then used to rapidly compute the numerical value of that specific eigenvalue with a desired accuracy. It is possible to efficiently accommodate the contribution of the imaginary eigenvalues hence eliminating occurrence of numerical instabilities as the number of terms in a series solution becomes large.

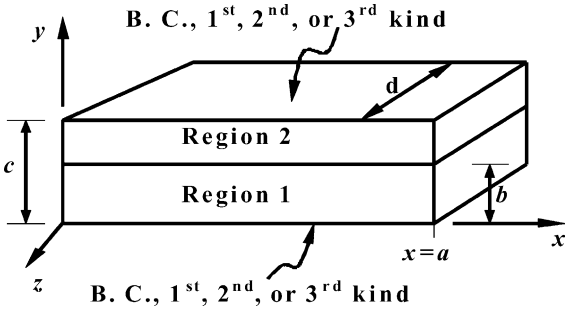

Fig. 1. Schematic of a two-layer body selected for this study.

Steady-state solutions complement transient solutions. However, in some cases transient solutions can enhance the accuracy and efficiency of steady-state solutions [2,13,14]. This topic is beyond the scope of the present paper.

The basic geometry considered in this paper is for two layers of different materials one above the other in the y-direction as shown in Fig. 1. The first material is in Region 1 which has a thickness in the y-direction of b, length in the x-direction of a, and in the z-direction of d. The second material is in Region 2 and has a thickness of c–b in the y-direction. Both materials can be orthotropic; that is, the thermal conductivities in the x-, y- and z-directions can be different in a given region. Furthermore, a thermal contact resistance is at the interface between the two materials. Perfect thermal contact is treated by letting the contact resistance be zero.

It is generally acceptable to use superposition of the temperature solution to solve the problem in two simpler parts: In the present problem, the first part considers nonhomogeneous boundary conditions at $y = 0$ and/or $y = c$ while all other boundary conditions are homogeneous. In the second part, the boundary conditions at $y = 0$ and/or $y = c$ are homogeneous while other boundary conditions could be nonhomogeneous. Accordingly, the mathematical formulations presented here also consist of two parts. The solution having nonhomogeneous boundary conditions along $y = 0$ and/or $y = c$ surfaces follows a standard solution technique; a brief presentation is provided for the sake of completeness. The emphasis of this work is directed toward the case when one or more nonhomogeneous boundary conditions exist along the surfaces $x = 0$ and a, and $z = 0$ and d.

2. Temperature solutions

The diffusion equation for orthotropic Regions 1 and 2 takes the following forms

$$k_{1x}\frac{\partial^2 T_1}{\partial x^2} + k_{1y}\frac{\partial^2 T_1}{\partial y^2} + k_{1z}\frac{\partial^2 T_1}{\partial z^2} = 0 \quad \text{in Region 1} \tag{1a}$$

$$k_{2x}\frac{\partial^2 T_2}{\partial x^2} + k_{2y}\frac{\partial^2 T_2}{\partial y^2} + k_{2z}\frac{\partial^2 T_2}{\partial z^2} = 0 \quad \text{in Region 2} \tag{1b}$$

The boundary conditions for specific cases are considered later. Using the method of separation of variables, one can set

$$T_1(x,y,z,t) = X_1(x)Y_1(y)Z_1(z) \quad \text{in Region 1} \tag{2a}$$

and

$$T_2(x,y,z,t) = X_2(x)Y_2(y)Z_2(z) \quad \text{in Region 2} \tag{2b}$$

In order to separate variables, the compatibility condition at $y = b$ requires that $X_1 = X_2$ and $Y_1 = Y_2$. Following substitution of T_1 from Eq. (2a) in Eq. (1a) and T_2 from Eq. (2b) in Eq. (1b), the result is

$$k_{1x}\frac{X_1''}{X_1} + k_{1y}\frac{Y_1''}{Y_1} + k_{1z}\frac{Z_1''}{Z_1} = 0 \quad \text{in Region 1} \tag{3a}$$

$$k_{2x}\frac{X_2''}{X_2} + k_{2y}\frac{Y_2''}{Y_2} + k_{2z}\frac{Z_2''}{Z_2} = 0 \quad \text{in Region 2} \tag{3b}$$

As stated earlier, the solutions for these equations when a nonhomogeneous boundary condition is located over $y = 0$ or $y = c$ surface is markedly different from a solution that uses a nonhomogeneous boundary condition over any other surface. Accordingly, there are two basic solutions; each is discussed separately.

2.1. Nonhomogeneous condition over $y = c$ surface

Solutions of this type have broad applications when designing heat spreaders for electronic devices. Typically, it is possible to have a discontinuous heat flux function at, e.g., $y = c$ surface simulating heat flux leaving different devices. A convective boundary condition over the $y = 0$ surface hints toward the existence of a cooling fluid or a heat sink system. Boundary conditions of the first or second kinds are possible on the $x = 0, a$ and $z = 0, d$ surfaces but not the third kind (Boundary conditions of the first kind denote prescribed temperatures, second kind denote prescribed heat flux and the third kind prescribed ambient temperatures in a convection condition.).

In this derivation, X_1, X_2, Z_1, and Z_2 in Eqs. (2a) and (2b) should satisfy the conditions:

$$X_1''/X_1 = X_2''/X_2 = -\beta^2 \tag{4a}$$

$$Z_1''/Z_1 = Z_2''/Z_2 = -v^2 \tag{4b}$$

whose solutions are

$$X_1 = X_2 = E\cos(\beta x) + F\sin(\beta x) \tag{4c}$$

$$Z_1 = Z_2 = G\cos(vz) + H\sin(vz) \tag{4d}$$

where β and v are eigenvalues depending on the specific type of homogeneous boundary conditions. Differential

equations for Y_1 and Y_2 can be obtained following substitution for T_1 and T_2 in the appropriate forms of the diffusion equation,

$$\begin{cases} -k_{1x}\beta^2 + k_{1y}Y_1''/Y_1 - k_{1z}v^2 = 0 \\ -k_{2x}\beta^2 + k_{2y}Y_2''/Y_2 - k_{2z}v^2 = 0 \end{cases} \tag{5}$$

that yields

$$\begin{cases} \dfrac{Y_1''}{Y_1} = \dfrac{k_{1x}}{k_{1y}}\beta^2 + \dfrac{k_{1z}}{k_{1y}}v^2 = \gamma^2 \\ \dfrac{Y_2''}{Y_2} = \dfrac{k_{2x}}{k_{2y}}\beta^2 + \dfrac{k_{2z}}{k_{2y}}v^2 = \eta^2 \end{cases} \tag{6}$$

As a shorthand notation, one can set $r_i = \sqrt{k_{ix}/k_{iy}}$, and $s_i = \sqrt{k_{iz}/k_{iy}}$ for $i = 1$ or 2.

The values of γ and η are obtainable by the relations

$$\gamma^2 = r_1^2\beta^2 + s_1^2v^2 \tag{7a}$$

$$\eta^2 = r_2^2\beta^2 + s_2^2v^2 \tag{7b}$$

The solutions for Y_1 and Y_2 functions are

$$\begin{cases} Y_1 = A\cosh(\gamma y) + B\sinh(\gamma y) \\ Y_2 = C\cosh(\eta y) + D\sinh(\eta y) \end{cases} \tag{8}$$

An alternative form of Y_2 is

$$Y_2 = \overline{C}\cosh[\eta(y-b)] + \overline{D}\sinh[\eta(y-b)] \tag{8a}$$

The boundary condition of the first kind at $y = 0$ makes $A = 0$ while the boundary condition of the second kind at $y = 0$ makes $B = 0$. The boundary condition of the third kind leads to a relation between A and b. Table 1 contains the values of A and b wherein a nonzero constant is set equal to unity. The compatibility conditions at the interface, $y = b$, are

$$-k_{1y}\partial T_1/\partial y|_{y=b} = (T_1 - T_2)|_{y=b}/R \tag{9a}$$

$$k_{1y}\partial T_1/\partial y|_{y=b} = k_{2y}\partial T_2/\partial y|_{y=b} \tag{9b}$$

The coefficients $\overline{C}$ and $\overline{D}$ for the boundary conditions of the first, second, and third kinds at $y = 0$ are given in Table 1. The notation J in the first column of this table implies that there is a nonhomogeneous boundary condition of the Jth kind at $y = c$.

Based on Eqs. (4a) and (4b), $X = X_1 = X_2$ and $Z = Z_1 = Z_2$. The eigenfunctions x and z depend on the homogeneous boundary conditions over the respective surfaces to produce the eigenvalues β_m and v_n. These solutions are designated as $X_m(\beta_m x)$ and $Z_n(v_n z)$. Since in Eqs. (7a) and (7b) γ and η also depend on both β_m and v_n, they are identified as γ_{mn} and v_{mn}. Once X_m, $Y_{1,mn}$, $Y_{2,mn}$, and Z_n are in hand, the temperature solutions take the following forms

$$T_1(x,y,z) = \sum_{m=1}^{\infty}\sum_{n=1}^{\infty} A_{mn}X_m(\beta_m x)Z_n(v_n z)Y_{1,mn}(\gamma_{mn} y) \tag{10a}$$

$$T_2(x,y,z) = \sum_{m=1}^{\infty}\sum_{n=1}^{\infty} A_{mn}X_m(\beta_m x)Z_n(v_n z)Y_{2,mn}(\eta_{mn} y) \tag{10b}$$

It is to be emphasized that the functions $X_m(\beta_m x)$ and $Z_n(v_n z)$ are solutions of Eqs. (4a) and (4b) for boundary conditions of first and second kind. Therefore, they have the form of sine and cosine. Consider now the case for a continuous or sectionally continuous heat flux $q(x,c,z) = -k_2(y)\partial T_2/\partial y$ over the $z = c$ surface,

$$\begin{aligned} q(x,c,z) &= q_0(x,z) \\ &= -k_{2y}\sum_{m=1}^{\infty}\sum_{n=1}^{\infty} A_{mn}X_m(\beta_m x)Z_n(v_n z)\eta_{mn}Y'_{2,mn}(\eta_{mn}c) \end{aligned} \tag{11}$$

The orthogonality conditions in the x- and z-directions suggest

$$\begin{aligned} A_{mn} = \frac{1}{k_{2y}N_{x,m}N_{z,n}}\frac{-1}{\eta_{mn}Y'_{2,mn}(c)} \\ \times \int_{z=0}^{d}\int_{x=0}^{a} q_0(x',z')X_m(\beta_m x')Z_n(v_n z')\,\mathrm{d}x'\,\mathrm{d}z' \end{aligned} \tag{12}$$

where

$$N_{x,m} = \int_0^a [X_m(\beta_m x)]^2\,\mathrm{d}x \tag{13}$$

$$N_{z,n} = \int_0^d [Z_n(v_n z)]^2\,\mathrm{d}z \tag{14}$$

The temperature solutions having boundary condition of the second kind at $y = c$ are

Table 1
Solution coefficients for steady-state heat conduction in two layers when $Y_1 = A\cosh(\gamma y) + B\sinh(\gamma y)$ and $Y_2 = \overline{C}\cosh[\eta(y-b)] + \overline{D}\sinh[\eta(y-b)]$

Case [9]	A	B	$\overline{C}$	$\overline{D}$
$Y1J$[a]	0	1	$\sinh(\gamma b) + k_{1y}R\gamma\cosh(\gamma b)$	$+(\gamma/\eta)(k_{1y}/k_{2y})\cosh(\gamma b)$
$Y2J$	1	0	$\cosh(\gamma b) + k_{1y}R\gamma\sinh(\gamma b)$	$(\gamma/\eta)(k_{1y}/k_{2y})\sinh(\gamma b)$
$Y3J$	1	$h_1/k_{1y}\gamma$	$\cosh(\gamma b) + h_1/(k_{1y}\gamma)\sinh(\gamma b)$ $+k_{1y}R\gamma[(h_1/k_{1y}\gamma)\cosh(\gamma b)+\sinh(\gamma b)]$	$(k_{1y}/k_{2y})(\gamma/\eta)[(h_1/k_{1y}\gamma)\cosh(\gamma b)$ $+\sinh(\gamma b)]$

[a] J stands for a boundary condition of the first, second, or third kind at $y = c$.

$$T_1(x,y,z) = -\sum_{m=1}^{\infty}\sum_{n=1}^{\infty}\frac{X_m(\beta_m x)Z_n(v_n z)}{k_{2y}N_{x,m}N_{z,n}} \times \frac{Y_{1,mn}(\gamma_{mn}y)}{\eta_{mn}Y'_{2,mn}(\eta_{mn}c)} \times \int_{z=0}^{d}\int_{x=0}^{a} q_0(x',z')X_m(\beta_m x')Z_n(v_n z')\,\mathrm{d}x'\,\mathrm{d}z' \tag{15a}$$

$$T_2(x,y,z) = -\sum_{m=1}^{\infty}\sum_{n=1}^{\infty}\frac{X_m(\beta_m x)Z_n(v_n z)}{k_{2y}N_{x,m}N_{z,n}} \times \frac{Y_{2,mn}(\eta_{mn}y)}{\eta_{mn}Y'_{2,mn}(\eta_{mn}c)} \times \int_{z=0}^{d}\int_{x=0}^{a} q_0(x',z')X_m(\beta_m x')Z_n(v_n z')\,\mathrm{d}x'\,\mathrm{d}z' \tag{15b}$$

Based on the classical approach [9, Appendix X], $X_m(\beta_m x) = \sin(\beta_m x)$ for a boundary condition of the first kind at $x = 0$. Similarly, $X_m(\beta_m x) = \cos(\beta_m x)$ for a boundary condition of the second kind at $x = 0$. In a similar line of reasoning, $Z_n(v_n z) = \sin(v_m z)$ or $Z_n(v_n z) = \cos(v_m z)$ for the boundary conditions of the first kind or the second kind at $z = 0$, respectively. Moreover, β_m depends on the type of boundary conditions at $x = a$, and v_n depends on the type of boundary conditions at $z = d$.

Consideration is given to a two-layer body each isotropic with perfect contact, as shown in Fig. 1, having $k_2/k_1 = 1/3$, $d/a = 1$, $c/a = 1/2$, and $b/a = 1/4$. The surface at $y = 0$ is exposed to a convective boundary condition with $ha/k_1 = 1/4$ and there is a prescribed heat flux q_0 over the $y = c$ surface extending from $x = 0$ to $x = a_1$ and from $z = 0$ to $z = d_1$ while all other surfaces are insulated. Eq. (15b) produced the following results for different heated regions $a_1/a = d_1/d = 0.1$, 0.25, 0.5, and 1.0 the computed dimensionless hot spot temperatures are $k_1(T - T_\infty)/(aq_0) = 0.3399081$, 0.8738421, 1.9183105, and 5, respectively. Using this approach, a relatively large number of terms were used to acquire these data. For a higher accuracy with a smaller number of terms, alternative methods [2,9,14] are available; e.g., time partitioning [9] can provide a higher accuracy with a fewer terms.

2.2. Nonhomogeneous condition over $x = a$ surface

Solutions to problems with the specified nonhomogeneous boundary conditions at $x = a$ require special attention. Computation of the eigenvalues often requires iteration and the orthogonality condition has its unique features. To illustrate the solution method, consideration is given to the case when temperature is known over the $x = a$ surface. Then, only minor modifications can produce solutions to problems with other boundary conditions. When using Eqs. (3a) and (3b), one can set

$$Y_1''/Y_1 = -\gamma^2 \tag{16a}$$

$$Y_2''/Y_2 = -\eta^2 \tag{16b}$$

$$Z_1''/Z_1 = Z_2''/Z_2 = -v^2 \tag{16c}$$

and

$$X_1''/X_1 = X_2''/X_2 = \beta^2 \tag{16d}$$

After substitution, this yields the relations

$$\gamma^2 = \frac{k_{1x}}{k_{1y}}\beta^2 - \frac{k_{1z}}{k_{1y}}v^2 = r_1^2\beta^2 - s_1^2v^2 \tag{17a}$$

$$\eta^2 = \frac{k_{2x}}{k_{2y}}\beta^2 - \frac{k_{2z}}{k_{2y}}v^2 = r_2^2\beta^2 - s_2^2v^2 \tag{17b}$$

Note that for isotropic materials, $r_1 = s_1 = 1$ and $r_2 = s_2 = 1$, then $\gamma^2 = \beta^2 - v^2 = \eta^2$.

The solutions for Y_1 and Y_2 are

$$Y_1 = A\cos(\gamma y) + B\sin(\gamma y) \tag{18a}$$

$$Y_2 = C\cos(\eta y) + D\sin(\eta y) = \overline{C}\cos[\eta(y-b)] + \overline{D}\sin[\eta(y-b)] \tag{18b}$$

and the solution for $Z = Z_1 = Z_2$ remains as given in Eq. (4d). The solutions for $X = X_1 = X_2$ is

$$X = E\cosh(\beta x) + F\sinh(\beta x) \tag{19}$$

The coefficients A and B for each of the boundary conditions of the first, second and third kind at $y = 0$ are listed in Table 2. The coefficients $\overline{C}$ and $\overline{D}$ that satisfy the compatibility conditions at $y = b$ are also listed in Table 2. Moreover, the boundary condition at $y = c$, provides the eigenconditions as described in the transient solution [6]. Table 3 lists the eigenconditions for nine different combinations of the boundary conditions at $y = 0$ and $y = c$.

As a prelude to the computation of temperature, the calculation of eigenvalues for the y-direction is the major task. The computation of eigenvalues follows a similar procedure as described for the transient problems by Haji-Sheikh and Beck [6], except, γ and η are now related to each other differently (see Eqs. (17a) and (17b)). A sample of a numerical scheme to compute the eigenvalues is given in Ref. [6]. According to Eqs. (17a) and (17b), it is possible to have $s_1^2v^2 > r_1^2\beta^2$ or $s_2^2v^2 > r_2^2\beta^2$, thereby making γ or η imaginary. Following the computation of eigenvalues from an appropriate transcendental equation in Table 3, the temperature solutions in Regions 1 and 2 are given by a relation similar to Eqs. (10a) and (10b); however, the eigenfunctions are different,

$$T_1(x,y,z) = \sum_{p=1}^{\infty}\sum_{n=1}^{\infty} A_{np}X_{np}(\beta_{np}x)Z_n(v_n z)Y_{1,np}(\gamma_{np}y) \tag{20a}$$

Table 2
Solution coefficient with contact resistance for $Y_1 = A\cos(\gamma y) + B\sin(\gamma y)$ and $Y_2 = \overline{C}\cos[\eta(y-b)] + \overline{D}\sin[\eta(y-b)]$

Case [9]	A	B	$\overline{C}$	$\overline{D}$
$Y1J$[a]	0	1	$\sin(\gamma b) + k_{1y}R\gamma\cos(\gamma b)$	$(\gamma/\eta)(k_{1y}/k_{2y})\cos(\gamma b)$
$Y2J$	1	0	$\cos(\gamma b) - k_{1y}R\gamma\sin(\gamma b)$	$-(\gamma/\eta)(k_{1y}/k_{2y})\sin(\gamma b)$
$Y3J$	1	$h_1/k_{1y}\gamma$	$\cos(\gamma b) + h_1/(k_{1y}\gamma)\sin(\gamma b)$ $+ k_{1y}R\gamma[(h_1/k_{1y}\gamma)\cos(\gamma b) - \sin(\gamma b)]$	$(k_{1y}/k_{2y})(\gamma/\eta)[(h_1/k_{1y}\gamma)\cos(\gamma b)$ $-\sin(\gamma b)]$

[a] J stands for a boundary condition of the first, second, or third kind at $y = c$.

Table 3
Eigenconditions for $Y11$, $Y12$, $Y13$, $Y21$, $Y22$, $Y23$, $Y31$, $Y32$, and $Y33$ cases

$Y11$	$\cot(\overline{\eta}) = -\left(\frac{c-b}{b}\right)\left(\frac{\overline{\gamma}}{\overline{\eta}}\right)\left(\frac{k_{1y}}{k_{2y}}\right)\frac{\cot(\overline{\gamma})}{1+R_b\overline{\gamma}\cot(\overline{\gamma})}$
$Y12$	$\tan(\overline{\eta}) = \left(\frac{c-b}{b}\right)\left(\frac{\overline{\gamma}}{\overline{\eta}}\right)\left(\frac{k_{1y}}{k_{2y}}\right)\frac{\cot(\overline{\gamma})}{1+R_b\overline{\gamma}\cot(\overline{\gamma})}$
$Y13$	$\frac{\overline{\eta}\tan(\overline{\eta}) - Bi_2}{(Bi_2 - R_c\overline{\eta}^2)\tan(\overline{\eta}) + \overline{\eta}(1+R_cBi_2)} = \left(\frac{c-b}{b}\right)\left(\frac{\overline{\gamma}}{\overline{\eta}}\right)\left(\frac{k_{1y}}{k_{2y}}\right)\cot(\overline{\gamma})$
$Y21$	$\cot(\overline{\eta}) = \left(\frac{c-b}{b}\right)\left(\frac{\overline{\gamma}}{\overline{\eta}}\right)\left(\frac{k_{1y}}{k_{2y}}\right)\frac{\tan(\overline{\gamma})}{1-R_b\overline{\gamma}\tan(\overline{\gamma})}$
$Y22$	$\tan(\overline{\eta}) = -\left(\frac{c-b}{b}\right)\left(\frac{\overline{\gamma}}{\overline{\eta}}\right)\left(\frac{k_{1y}}{k_{2y}}\right)\frac{\tan(\overline{\gamma})}{1-R_b\overline{\gamma}\tan(\overline{\gamma})}$
$Y23$	$\frac{\overline{\eta}\tan(\overline{\eta}) - Bi_2}{(Bi_2 - R_c\overline{\eta}^2)\tan(\overline{\eta}) + \overline{\eta}(1+R_cBi_2)} = -\left(\frac{c-b}{b}\right)\left(\frac{\overline{\gamma}}{\overline{\eta}}\right)\left(\frac{k_{1y}}{k_{2y}}\right)\tan(\overline{\gamma})$
$Y31$	$\cot(\overline{\eta}) = \left(\frac{c-b}{b}\right)\left(\frac{\overline{\gamma}}{\overline{\eta}}\right)\left(\frac{k_{1y}}{k_{2y}}\right)\frac{\overline{\gamma}\tan(\overline{\gamma}) - Bi_1}{(Bi_1 - R_b\overline{\gamma}^2)\tan(\overline{\gamma}) + \overline{\gamma}(1+R_bBi_1)}$
$Y32$	$\tan\overline{\eta} = -\left(\frac{c-b}{b}\right)\left(\frac{\overline{\gamma}}{\overline{\eta}}\right)\left(\frac{k_{1y}}{k_{2y}}\right)\frac{\overline{\gamma}\tan(\overline{\gamma}) - Bi_1}{(Bi_1 - R_b\overline{\gamma}^2)\tan(\overline{\gamma}) + \overline{\gamma}(1+R_bBi_1)}$
$Y33$	$\frac{\overline{\eta}\tan(\overline{\eta}) - Bi_2}{Bi_2\tan(\overline{\eta}) + \overline{\eta}} = -\left(\frac{c-b}{b}\right)\left(\frac{\overline{\gamma}}{\overline{\eta}}\right)\left(\frac{k_{1y}}{k_{2y}}\right)\frac{\overline{\gamma}\tan(\overline{\gamma}) - Bi_1}{(Bi_1 - R_b\overline{\gamma}^2)\tan(\overline{\gamma}) + \overline{\gamma}(1+R_bBi_1)}$

The parameters γ and η are related by the relations $\gamma^2 = r_1^2\beta^2 - s_1^2v^2$ and $\eta^2 = r_2^2\beta^2 - s_2^2v^2$.
Notations: $\overline{\gamma} = \gamma b$, $\overline{\eta} = \eta(c-b)$, $Bi_1 = h_1b/k_{1y}$, $Bi_2 = h_2(c-b)/k_{2y}$, $R_b = Rk_{1y}/b$, $R_c = Rk_{2y}/(c-b)$, and R is defined so that $(T_1 - T_2)|_{y=b}/R = -k_{1y}.(\partial T/\partial y)|_{y=b}$.

$$T_2(x,y,z) = \sum_{p=1}^{\infty}\sum_{n=1}^{\infty} A_{np}X_{np}(\beta_{np}x)Z_n(v_nz)Y_{2,np}(\eta_{np}y) \tag{20b}$$

According to Eqs. (17)–(20), for each eigenvalue in the z-direction, there are two sets of eigenvalues: (v_n, γ_{np}) in Regions 1 and (v_n, η_{np}) in Region 2. The corresponding eigenfunctions for the y-direction are $Y_{1,np}(\gamma_{np}y)$ in Region 1 and $Y_{2,np}(\eta_{np}y)$ in Region 2. These eigenvalues provide β_{np} Eqs. (17a) and (17b) and the function $X_{np}(\beta_{np}x)$ for the x-directions. Next, the coefficient A_{mn} is obtained using a nonhomogeneous boundary condition, e.g., $T = T_1(a, y', z')$ at $x = a$. To utilize the boundary condition in subsequent computations, it is necessary to identify a required orthogonality condition. The derivation of the orthogonality condition peculiar to this steady-state solution is relatively extensive hence it is described separately, see Appendix A. To elucidate the algebraic steps leading to a solution, it is assumed that the temperature is prescribed over the $x = a$ surface. Then, the value of A_{np} for inclusion in Eqs. (20a) and (20b) is obtained using the orthogonality condition, Eq. (A.8), as

$$A_{np} = \frac{1}{N_{y,np}N_{z,n}}\frac{1}{X_{np}(\beta_{np}a)} \times \int_{z=0}^{d}\left[\int_{y=0}^{b} k_{1x}T_1(a,y',z')Y_{1,np}(\gamma_{np}y')\,dy' + \int_{y=b}^{c} k_{2x}T_2(a,y',z')Y_{2,np}(\eta_{np}y')\,dy'\right]Z_n(v_nz')\,dz' \tag{21}$$

Note that this orthogonality condition in Eq. (A.8) (in Appendix A) contains the thermal conductivity values as a weighting function and leads the following definitions of the norms

$$N_{y,np} = \int_{y=0}^{b} k_{1x}[Y_{1,np}(\gamma_{np}y)]^2\,\mathrm{d}y + \int_{y=b}^{c} k_{2x}[Y_{2,np}(\eta_{np}y)]^2\,\mathrm{d}y \tag{22a}$$

$$N_{z,n} = \int_{z=0}^{d} [Z_n(v_n z)]^2\,\mathrm{d}z \tag{22b}$$

When a homogeneous boundary condition is located over the $z = d$ surface, the solution is similar to the above with a minor modification of Eqs. (20)–(22); that is,

$$T_1(x,y,z) = \sum_{p=1}^{\infty}\sum_{m=1}^{\infty} A_{mp} Z_{mp}(v_{mp}z) X_m(\beta_m x) Y_{1,mp}(\gamma_{mp}y) \tag{23a}$$

$$T_2(x,y,z) = \sum_{p=1}^{\infty}\sum_{m=1}^{\infty} A_{mp} Z_{mp}(v_{mp}z) X_m(\beta_m x) Y_{2,mp}(\eta_{mp}y) \tag{23b}$$

After some modification, Eq. (21) yields the coefficient A_{mp} as

$$A_{mp} = \frac{1}{N_{y,mp}N_{x,m}}\frac{1}{Z_{mp}(v_{mp}d)} \times \int_{x=0}^{a}\left[\int_{y=0}^{b} k_{1z}T_1(x',y',d)Y_{1,mp}(\gamma_{mp}y')\,\mathrm{d}y' + \int_{y=b}^{c} k_{2z}T_2(x',y',d)Y_{2,mp}(\eta_{mp}y')\,\mathrm{d}y'\right] X_m(\beta_m x')\,\mathrm{d}x' \tag{24}$$

wherein the norms for the y- and x-directions, after a minor modification, are

$$N_{y,mp} = \int_{y=0}^{b} k_{1z}[Y_{1,mp}(\gamma_{mp}y)]^2\,\mathrm{d}y + \int_{y=b}^{c} k_{2z}[Y_{2,mp}(\eta_{mp}y)]^2\,\mathrm{d}y \tag{25a}$$

$$N_{x,m} = \int_{x=0}^{a} [X_m(\beta_m x)]^2\,\mathrm{d}x, \tag{25b}$$

At this point, it is appropriate to evaluate this methodology through a numerical example.

3. Numerical studies

Two numerical examples are selected in order to demonstrate the mathematical steps and provide a measure of the numerical accuracy. These examples are chosen because the heat flux distributions can be discontinuous at the interface; consequently, these are particularly challenging cases.

Example 1. Consideration is given to a case where the solid depicted in Fig. 1 has insulating walls at $y = 0$, $y = c$, $z = 0$, and $z = d$ while the surface at $x = 0$ is kept at temperature $T_1 = T_2 = 0$ and there is a prescribed heat flux over the $x = a$ surface. Therefore, Eq. (21) for inclusion in Eqs. (20a) and (20b) needs to be modified. Table 2 provides the eigenfunctions for the y-direction and Eq. (4d) provides the eigenfunction in the z-direction; that is, $Z_n(v_n z) = \cos(v_n z)$ with $v_n = n\pi/d$ and $n = 0, 1, 2, \ldots, \infty$. A solution, described by Eq. (19), that satisfies the homogeneous boundary condition at $x = 0$ is $X_{np}(\beta_{np}x) = \sinh(\beta_{np}x)$ in which β_{np} relates to n and γ_{np} in Region 1 and n and η_{np} in Region 2. Eqs. (20a) and (20b) provide the temperature solution, in Region 1 or 2, following appropriate substitutions as

$$T_1(x,y,z) = \sum_{p=1}^{\infty}\sum_{n=0}^{\infty} A_{np}\sinh(\beta_{np}x)\cos(n\pi z/d) \times \cos(\gamma_{np}y) \tag{26a}$$

$$T_2(x,y,z) = \sum_{p=1}^{\infty}\sum_{n=1}^{\infty} A_{np}\sinh(\beta_{np}x)\cos(n\pi z/d) \times \{\overline{C}_{np}\cos[\eta_{np}(y-b)] + \overline{D}_{np}\sin[\eta_{np}(y-b)]\} \tag{26b}$$

The function $Y_{2,np}$ is the entry $Y2J$ in Table 2 that contains the coefficients

$$\overline{C}_{np} = \cos(\gamma_{np}b) - k_{1y}R\gamma_{np}\sin(\gamma_{np}b) \tag{27a}$$

$$\overline{D}_{np} = -(\gamma_{np}/\eta_{np})(k_{1y}/k_{2y})\sin(\gamma_{np}b) \tag{27b}$$

The nonhomogeneous boundary condition at $x = a$ is

$$q_i(a,y',z') = -k_{ix}\left.\frac{\partial T_i}{\partial x}\right|_{x=a} \quad \text{for } i = 1 \text{ or } 2$$

that produces

$$q_1(x,y,z) = -\sum_{p=1}^{\infty}\sum_{n=0}^{\infty} A_{np}k_{1x}\beta_{np}\cosh(\beta_{np}x)\cos(n\pi z/d) \times \cos(\gamma_{np}y)$$

$$q_2(x,y,z) = -\sum_{p=1}^{\infty}\sum_{n=1}^{\infty} A_{np}k_{2x}\beta_{np}\cosh(\beta_{np}x)\cos(n\pi z/d) \times \{\overline{C}_{np}\cos[\eta_{np}(y-b)] + \overline{D}_{np}\sin[\eta_{np}(y-b)]\}$$

For a numerical study, consider the problem in which $q_1 = q_2 = q_0 = \text{constant}$, $d/a = 1$, $b/a = 1/4$, and $c/a = 1/2$. The coefficient A_{np} is obtainable using the orthogonality condition in Eq. (A.8); that yields,

$$A_{np} = \frac{1}{N_{y,np}N_{z,n}}\frac{-1}{\beta_{np}\cosh(\beta_{np}a)} \times \int_{z=0}^{d}\left[\int_{y=0}^{b} q_1\cos(\gamma_{np}y)\,\mathrm{d}y + \int_{y=b}^{c} q_2\{\overline{C}_{np}\cos[\eta_{np}(y-b)] + \overline{D}_{np}\sin[\eta_{np}(y-b)]\}\,\mathrm{d}y\right]\cos(n\pi z/d)\,\mathrm{d}z \tag{28}$$

wherein

$$N_{y,np} = \int_{y=0}^{b} k_{1x}[\cos(\gamma_{np}y)]^2\,\mathrm{d}y + \int_{y=b}^{c} k_{2x}\{\overline{C}_{np}\cos[\eta_{np}(y-b)] + \overline{D}_{np}\sin[\eta_{np}(y-b)]\}^2\,\mathrm{d}y \tag{29}$$

and

$$N_{z,n} = \int_{z=0}^{d}[\cos(n\pi z/d)]^2\,\mathrm{d}z = \begin{cases} d & \text{when } n=0 \\ d/2 & \text{when } n>0 \end{cases} \tag{30}$$

Since $q_1 = q_2 = q_0 = \text{constant}$ is independent of z, then the coefficient $A_{np} = 0$ when $n > 0$ because of the following term in Eq. (28)

$$\int_{z=0}^{d}\cos(n\pi z/d)\,\mathrm{d}z = \begin{cases} d & \text{when } n=0 \\ \frac{\sin(n\pi)}{n\pi/d} = 0 & \text{when } n>0 \end{cases} \tag{31}$$

and the problem becomes two-dimensional. Accordingly, the coefficients in Eqs. (28) and (29), when $\gamma_{np} > 0$ and $\eta_{np} > 0$, reduce to

$$A_{np} = \frac{-q_0}{N_{y,np}\beta_{np}\cosh(\beta_{np}a)} \times \left\{ \frac{\sin(\gamma_{np}b)}{\gamma_{np}} + \overline{C}_{np}\frac{\sin[\eta_{np}(c-b)]}{\eta_{np}} + \overline{D}_{np}\frac{1-\cos[\eta_{np}(c-b)]}{\eta_{np}} \right\} \tag{32}$$

and when $\gamma_{np} > 0$ and $\eta_{np} > 0$,

$$N_{y,np} = k_{1x}\left[\frac{b}{2} + \frac{1}{4\gamma_{np}}\sin(2\gamma_{np}b)\right] + k_{2x}\left\{\frac{1}{2}(\overline{C}_{np}^2 + \overline{D}_{np}^2) \times (c-b) + \frac{1}{2\eta_{np}}\overline{C}_{np}\overline{D}_{np}\{1-\cos[2\eta_{np}(c-b)]\} + \frac{1}{4\eta_{np}}(\overline{C}_{np}^2 - \overline{D}_{np}^2)\sin[2\eta_{np}(c-b)]\right\} \tag{33}$$

while the coefficient $\overline{C}_{np}$ and $\overline{D}_{np}$ are in Eqs. (27a) and (27b).

The eigenvalues for the y-direction are found from Table 3 using the entry $Y22$. The solution presented here is equally valid for orthotropic bodies, as the orthotropic effects should be considered when computing the eigenvalues and when using the boundary condition of the second kind or third kind. In this numerical example, consideration is given to a special case when $b = c - b$ and materials are isotropic. This condition leads to some simplification, that is, $\overline{\gamma} = \overline{\eta}$ and $\tan(\overline{\gamma}) = \tan(\overline{\eta})$. According to the $Y22$ eigencondition in Table 3, there are two sets of eigenvalues. The members of both sets are the roots of equation

$$[1 - R_b\overline{\gamma}_b\tan(\overline{\gamma}_p)]\tan(\overline{\gamma}_p) = -\frac{k_1}{k_2}\tan(\overline{\gamma}_p) \tag{34}$$

which yields the two conditions of

$$\overline{\gamma}_p\tan(\overline{\gamma}_p) = \frac{1}{R_b}\frac{k_1+k_2}{k_2} \quad \text{for } p = 1,2,3,\ldots \tag{35a}$$

$$\cos(\overline{\gamma}_p) = 0 \quad \text{for } p = 1,2,3,\ldots \tag{35b}$$

The eigencondition given by Eq. (35a) is the same as for the $X23$ (or $X32$) [9] case.From Eqs. (35a) and (35b) which imply $b = cb$, isotropic materials and $R_b = 0$, the first set of eigenvalues is

$$\overline{\gamma}_p = (2p-1)\pi/2 \quad \text{for } p = 1,2,3,\ldots \tag{36}$$

The second set of eigenvalues is

$$\overline{\gamma}_p = (p-1)\pi, \quad p = 1,2,3,\ldots \tag{37}$$

Therefore, in this example there are two sets of eigenvalues to be incorporated in the temperature solution; recall for this example that, $\overline{\gamma} = \overline{\eta} = \overline{\beta}$.

Because of the integral in Eq. (31), only the term $p = 1$ from the second set contributes to the solution; therefore, after replacing A_{np} by A_p and as $\overline{\gamma}_p \to 0$, the value of $A_p\sinh(\gamma_p x)$ becomes

$$\begin{aligned}\lim_{p\to 1}[\sinh(\overline{\gamma}_p x/b)A_p] &= \lim_{\overline{\gamma}_p\to 0}\left[\frac{\sinh(\overline{\gamma}_p x/b)}{\overline{\gamma}_p/b}\right]\frac{-q_0}{N_{y,1}}\left\{\frac{\sin(\gamma_p b)}{\overline{\gamma}_p/b} + \overline{C}_{np}\frac{\sin[\overline{\gamma}_p(c-b)/b]}{\overline{\gamma}_p/b} + \overline{D}_{np}\frac{1-\cos[\overline{\gamma}_p(c-b)/b]}{\overline{\gamma}_p/b}\right\} \\ &= \frac{-q_0 x}{N_{y,1}}[b + \overline{C}_p(c-b)] \\ &= \frac{-2q_0 bx}{N_{y,1}}\end{aligned} \tag{38}$$

In this limiting quantity, $c - b = b$ and for the second set of eigenvalues given by Eq. (37), when $p = 1$, $\overline{\gamma}_p = 0$ and using Eqs. (27a) and (27b), one gets $\overline{C}_{np} = \overline{C}_p = \cos(\overline{\gamma}_p) = 1$ and $\overline{D}_{np} = \overline{D}_p = 0$. For the first set of eigenvalues given by Eq. (36), A_p is

$$A_p = \frac{-q_0 b^2}{N_{y,p}\overline{\gamma}_p\cosh(\overline{\gamma}_p a/b)} \times \left\{\frac{\sin(\overline{\gamma}_p)}{\overline{\gamma}_p} + \overline{C}_p\frac{\sin[\overline{\gamma}_p(c-b)/b]}{\overline{\gamma}_p} + \overline{D}_p\frac{1-\cos[\overline{\gamma}_p(c-b)/b]}{\overline{\gamma}_p}\right\} \tag{39}$$

Moreover, the coefficients for the first set of eigenvalues, using $\cos(\overline{\gamma}_p) = 0$ and $R = 0$, reduce to

$$\overline{C}_{np} = \overline{C}_p = 0 \tag{40a}$$

$$\overline{D}_{np} = \overline{D}_p = -(k_1/k_2)\sin(\gamma_{np}b) \tag{40b}$$

For $(c-b)=b$, following substitution for $\overline{C}_{np}$ and $\overline{D}_{np}$ from Eqs. (40a) and (40b) in Eq. (32), one obtains

$$A_p=\frac{-q_0b^2}{N_{y,p}\overline{\gamma}_p\cosh(\overline{\gamma}_pa/b)}\frac{\sin(\overline{\gamma}_p)}{\overline{\gamma}_p}[1-(k_1/k_2)\sin(\overline{\gamma}_p)] \tag{41}$$

Eq. (29), following integration and substitution of $\overline{C}_{np}$ and $\overline{D}_{np}$, yields the y-direction norms for the second set of eigenvalues as $N_{y,p}=b(k_1+k_2)$ when $p=1$ and

$$N_{y,p}=k_1\frac{b}{2}+k_2\left[\frac{b}{2}+\frac{b}{4\overline{\gamma}_p}\sin(2\overline{\gamma}_p)\right] \tag{42}$$

when $p>1$. Since the sine term in the above Eq. (42) vanishes for all values of $p>1$, then

$$N_{y,p}=\begin{cases}b(k_1+k_2), & \text{when } p=1\\ \frac{b}{2}(k_1+k_2), & \text{when } p>1\end{cases} \tag{43}$$

For the first set of eigenvalues, when $c-b=b$ and $R=0$, the norm for the y-direction reduces to

$$N_{y,p}=\frac{bk_1}{2}[1+(k_1/k_2)] \tag{44}$$

From the above equations the temperatures in Regions 1 and 2 for the special case of $b=cb$ and for isotropic materials in perfect contact, $R=0$, the temperatures are

$$T_1(x,y)=\frac{-2q_0b}{k_1+k_2}\left\{\frac{x}{b}+\left(\frac{k_2}{k_1}-1\right)\times\sum_{p=1}^{\infty}\left[\frac{\sin(\overline{\gamma}_p)\cos(\overline{\gamma}_py/b)\sinh(\overline{\gamma}_px/b)}{(\overline{\gamma}_p)^2\cosh(\overline{\gamma}_pa/b)}\right]\right\} \tag{45}$$

$$T_2(x,y)=\frac{-2q_0b}{k_1+k_2}\left\{\frac{x}{b}-\left(\frac{k_2}{k_1}-1\right)\times\sum_{p=1}^{\infty}\left[\frac{k_1\sin[\overline{\gamma}_p(y-b)/b]\sinh(\overline{\gamma}_px/b)}{k_2(\overline{\gamma}_p)^2\cosh(\overline{\gamma}_pa/b)}\right]\right\} \tag{46}$$

where, in Eq. (46), the quantity $\sin[\overline{\gamma}_p(y-b)/b]$ reduces to $\sin(\overline{\gamma}_p)\cos(\overline{\gamma}_py/b)$ using the eigenvalues given by Eq. (36). Then Eq. (46) becomes

$$T_2(x,y)=\frac{-2q_0b}{k_1+k_2}\left\{\frac{x}{b}-\left(1-\frac{k_1}{k_2}\right)\times\sum_{p=1}^{\infty}\left[\frac{(-1)^p\cos(\overline{\gamma}_py/b)\sinh(\overline{\gamma}_px/b)}{(\overline{\gamma}_p)^2\cosh(\overline{\gamma}_pa/b)}\right]\right\} \tag{47}$$

The negative sign in front of Eqs. (45) and (46) implies that positive heat flux flows in the direction of the x-axis; that is, positive if leaving and negative if entering this body at $x=a$. Furthermore, for this special case, the temperature over the $y=b$ surface changes linearly with x.

Using the eigenvalues given by Eq. (36) and the transformed y variable of $y'=y-b$, the temperature distribution given by Eqs. (45) and (46) can be written as

$$\frac{T(x,y')}{q_0a/[(k_1+k_2)/2]}=-\begin{cases}\dfrac{x}{a}-\dfrac{k_2-k_1}{k_1}\dfrac{b}{a}S_s\left(\dfrac{x}{a},\dfrac{y'}{b};\dfrac{a}{b}\right), & -b\leqslant y'\leqslant 0\\ \dfrac{x}{a}-\dfrac{k_2-k_1}{k_2}\dfrac{b}{a}S_s\left(\dfrac{x}{a},\dfrac{y'}{b};\dfrac{a}{b}\right), & 0\leqslant y'\leqslant b\end{cases} \tag{48a}$$

where

$$S_s\left(\frac{x}{a},\frac{y'}{b};\frac{a}{b}\right)=\sum_{p=1}^{\infty}\frac{\sin(\overline{\gamma}_py'/b)}{(\overline{\gamma}_p)^2}\left[\frac{\sinh(\overline{\gamma}_px/b)}{\cosh(\overline{\gamma}_pa/b)}\right]=\sum_{p=1}^{\infty}\frac{\sin(\overline{\gamma}_py'/b)}{(\overline{\gamma}_p)^2}\left[\frac{e^{-\overline{\gamma}_p(a-x)/b}-e^{-\overline{\gamma}_p(a+x)/b}}{1+e^{-2\overline{\gamma}_pa/b}}\right] \tag{48b}$$

and T stands for T_1 or T_2. The notation S_s has a subscript s to denote the presence of the sinh function in the numerator. Notice that S_s is equal to zero at $x=0$ and also at $y'=0$; that is,

$$S_s\left(0,\frac{y'}{b};\frac{a}{b}\right)=0 \quad \text{and} \quad S_s\left(\frac{x}{a},0;\frac{a}{b}\right)=0 \tag{49a}$$

The first of these relations describes the imposed boundary condition at $x=0$. The second one shows that the temperature distribution is linear in x and it is given by

$$\frac{T(x,0)}{q_0a/[(k_1+k_2)/2]}=-\frac{x}{a} \tag{49b}$$

Another important observation is that

$$S_s\left(\frac{x}{a},-\frac{y'}{b};\frac{a}{b}\right)=-S_s\left(\frac{x}{a},\frac{y'}{b};\frac{a}{b}\right) \tag{49c}$$

This relationship permits ready evaluation of the S_s function for negative values of y'. Hence, the S_s function need be plotted only for positive arguments. Furthermore, S_s describes the anti-symmetric component within the temperature distribution about $y'=0$.

The exponential form of S_s (see Eq. (48b)) can be used to determine the required number of terms in the series, provided $x\neq a$. The largest and most important of the exponential terms is $\exp[-\overline{\gamma}_p(a-x)/b]$ which is less than 10^{-5} if

$$(\overline{\gamma}_p)_{\max}\frac{a-x}{b}=2(p_{\max}-1)\frac{\pi}{2}\frac{a-x}{b}<11.5 \tag{50a}$$

and thus

$$p_{\max}\approx 3.66\frac{b}{a-x}+\frac{1}{2}=3.66\frac{b/a}{1-x/a}+\frac{1}{2} \tag{50b}$$

For the exponential term less than 10^{-10}, the coefficient 3.66 is doubled to about 7.33. Notice as x approaches a, the number of terms increases dramatically. However, for $x = 0.95a$ and $b = a/4$, the maximum number of terms in S_s to have an error less than about one part in 10^{-10} is 19. Actually fewer terms would be necessary but this is a convenient equation to use. At $x = a$, an infinite number of terms would be required using the above equation.

Since this location is an important one, an alternative solution is given. For this special case, the transformations

$$T_1(x,y) = -q_0 x/k_1 + \theta_1(x,y) \tag{51a}$$

$$T_2(x,y) = -q_0 x/k_2 + \theta_2(x,y) \tag{51b}$$

shift the nonhomogeneous boundary condition from $x = a$ to $y = b$, thereby providing accurate solutions in both layers along the $x = a$ surface. Using the above transformations, which is beyond the scope of this presentation, the analogous solution is

$$\frac{T(x,y')}{q_0 a/k_1} = -\begin{cases} \dfrac{x}{a} - \dfrac{k_2-k_1}{k_1+k_2} S_{cR}\left(\dfrac{x}{a},\dfrac{y'}{b};\dfrac{a}{b},R^+\right), & -b \leqslant y' \leqslant 0 \\ \dfrac{k_1}{k_2}\left[\dfrac{x}{a} + \dfrac{k_2-k_1}{k_1+k_2} S_{cR}\left(\dfrac{x}{a},\dfrac{y'}{b};\dfrac{a}{b},R^+\right)\right], & 0 \leqslant y' \leqslant b \end{cases} \tag{52}$$

where

$$S_{cR}\left(\frac{x}{a},\frac{y'}{b};\frac{b}{a},R^+\right) = 2\sum_{p=1}^{\infty} \frac{(-1)^{p+1}\sin(\overline{\gamma}_p x/a)\cosh[(\overline{\gamma}_p b/a)(1-|y'|/b)]}{(\overline{\gamma}_p)^2[\overline{\gamma}_p R^+ \sinh(\overline{\gamma}_p b/a) + \cosh(\overline{\gamma}_p b/a)]}$$

$$= 2\sum_{p=1}^{\infty} \frac{(-1)^{p+1}\sin(\overline{\gamma}_p x/a)[e^{-\overline{\gamma}_p(b/a)|y'|/b} + e^{-\overline{\gamma}_p(b/a)(2-|y'|/b)}]}{(\overline{\gamma}_p)^2[\overline{\gamma}_p R^+(1-e^{-2\overline{\gamma}_p b/a}) + 1 + e^{-2\overline{\gamma}_p(b/a)}]} \tag{53a}$$

and

$$R^+ = \frac{k_2}{k_1+k_2}\frac{Rk_1}{a} \tag{53b}$$

In general, the solution converges quickly for $|y'|/a$ not being very small and it is the worst for $|y'|/a = 0$. In particular, it converges very well at $x = 0$, except when y' approaches zero. The maximum number of terms in the series is found in an analogous manner as Eq. (50b) and is

$$p_{max} \approx 3.66\frac{a}{b}\left|\frac{b}{y'}\right| + \frac{1}{2} = 3.66\frac{1}{(b/a)(|y'|/b)} + \frac{1}{2} \tag{54}$$

If $a/b = 4$ and $y' = b/20$, $p_{max} \approx 293$ which is not a large number for a single summation. In contrast, if $a/b = 0.25$ and $y' = b/20$, $p_{max} \approx 18$. The convergence characteristics of Eqs. (48b) and (53a) are quite different but they are complementary. This is demonstrated in Fig. 2 where the maximum number of terms p_{max} for S_s and S_c functions, at different values of b/a, is plotted as a function of x/a in Eq. (50b) and as a function of y'/b in Eq. (54). The convergence of S_s rapidly improves away from $x/a = 1$ and S_c away from $y'/b = 0$. In general S_s is better for small b/a values and S_c is better for large b/a values.

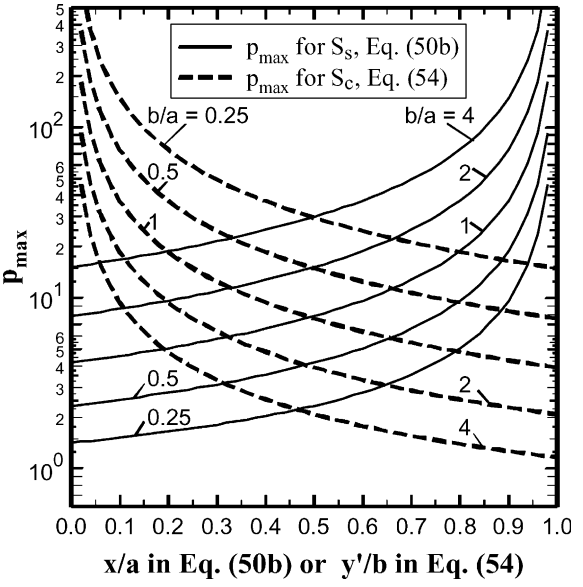

Fig. 2. Maximum number of terms, p_{max}, for S_s and S_c as functions of x/a in Eq. (50b) or y'/b in Eq. (54).

Since S_{cR} appears in both materials in the solution, it is instructive to examine it. First consider the case of perfect contact. Then S_{cR} becomes (denoted now S_c)

$$S_c\left(\frac{x}{a},\frac{y'}{b};\frac{b}{a}\right) = 2\sum_{p=1}^{\infty} \frac{(-1)^{p+1}\sin(\overline{\gamma}_p x/a)\cosh[(\overline{\gamma}_p b/a)(1-|y'|/b)]}{(\overline{\gamma}_p)^2\cosh(\overline{\gamma}_p b/a)]}$$

$$= 2\sum_{p=1}^{\infty} \frac{(-1)^{p+1}\sin(\overline{\gamma}_p x/a)[e^{-\overline{\gamma}_p(b/a)|y'|/b} + e^{-\overline{\gamma}_p(b/a)(2-|y'|/b)}]}{(\overline{\gamma}_p)^2[1+e^{-2\overline{\gamma}_p(b/a)}]} \tag{55}$$

Again the most slowly convergent location is at $y' = 0$; fortunately as shown below, that location has a simple algebraic expression.

Now, one can write two different expressions for the case of zero interface resistance. Equating Eqs. (48a) and (52) with S_{cR} replaced by S_c for the region of $0 < y' < b$ gives

$$-\frac{2}{k_1+k_2}\left[\frac{x}{a}-\frac{k_2-k_1}{k_1}\frac{b}{a}S_s\left(\frac{x}{a},\frac{y'}{b};\frac{a}{b}\right)\right] = -\frac{1}{k_2}\left[\frac{x}{a}-\frac{k_2-k_1}{k_1+k_2}S_c\left(\frac{x}{a},\frac{y'}{b};\frac{b}{a}\right)\right] \quad (56)$$

Solving for S_c gives

$$S_c\left(\frac{x}{a},\frac{y'}{b};\frac{b}{a}\right)=\frac{x}{a}-2\frac{b}{a}S_s\left(\frac{x}{a},\frac{y'}{b};\frac{b}{a}\right) \quad (57)$$

Using the second equation from Eq. (49a) in Eq (57) gives the simple algebraic expression (at the difficult location for Eq. (55) at $y'=0$) of

$$S_c\left(\frac{x}{a},0,\frac{b}{a}\right)=\frac{x}{a} \quad (58)$$

Eqs. (52) and (53) provide an alternative method of obtaining accurate temperature values along $x=a$.

For a numerical study, when $b/a=1/4$, $c/a=1/2$, and $k_2/k_1=2$, Fig. 3a shows the variation of dimensionless temperature $k_1T(x,y)/(aq_0)$ as a function of x and y. The data clearly show the temperature variation that is linear along $y=b$ and becomes nearly linear for all values of y when $(a-x)/a$ becomes larger than b/a. The heat flux component in the x-direction q_x/q_0, Fig. 3b, and the component in the y-direction, q_y/q_0, Fig. 3c, attest to this trend. Fig. 3c clearly shows that q_y/q_0 assumes a near zero value when $(a-x)/a>b/a$. In addition, Fig. 3b demonstrates that the heat flux component q_x/q_0 suffers a singularity at $y=b$ as x approaches a. Also, q_y/q_0 goes to infinity when $x=a$ and $y=b$ as shown in Fig. 3c.

Fig. 4 compares solutions provided by Eqs. (48a) and (52). The solid lines in Fig. 4a indicate the temperature values computed using Eq. (48a) and the dash lines with circular symbols are those using Eq. (52). Both solutions yield accurate results within the limitations demonstrated in Fig. 2. The circular symbols over a solid line imply that the dash line is hidden beneath the solid line. The computed values of q_x/q_0 are in Fig. 3b. They exhibit a unique feature, that is, a constant heat flux of $q_x/q_0=2/3$ in layer 1 and $q_x/q_0=4/3$ in layer 2, when $y/a=b/a=0.25$ for all values of x, see the first term in Eq. (47). This feature extends to $x=a$ at which, according to the boundary condition, q_x/q_0 must be equal to 1 in both layers, indicating an expected singularity. This singularity is also detectable in the q_y/q_0 data plotted in Fig. 3c. Therefore, the computed q_x/q_0 and q_y/q_0, in Fig. 3a and b, for both solutions show the effect of this singularity in the neighborhood of the intersection of $x=a$ plane and $y=b$ plane.

The convergence of temperature and flux component data is well within the guide lines graphically demonstrated in Fig. 2 except at the heated surface at $x=a$. Table 4 is prepared to demonstrate the rate of convergence of temperature at $x=a$ as the number of eigenvalues increases. The data assume perfect contact, $R=0$, and they show the convergence of the Fourier series solution in Eq. (48a), without the contribution of the exponentially decaying term, is relatively slow as the number of terms increases. For comparison, the temperature is also computed using Eq. (52) and it exhibits excellent convergence away from the $y=b$ plane. A comparison over a broader range of variables shows that these two solutions are nearly identical (see Fig. 4a–c).

In the presence of a contact resistance between layers, Eq. (35a) provides a set of eigenvalues and they should be computed numerically. The problem remains two-dimensional with $\overline{\gamma}=\overline{\eta}=\overline{\beta}$, except every term within the first and second set of eigenvalues, Eqs. (36) and (37), contributes to the solution. An extensive numerical study of the effect of contact resistance between the layers is in the next example.

Example 2. This example modifies the thermal conduction model studied in Example 1 in order to study the effect of contact resistance on the three-dimensional solution. By allowing the surface at $z=0$ to have a homogeneous boundary condition of the first kind instead of the second kind, the problem becomes three-dimensional with features similar to those in Example 1. The eigenfunction that satisfies the homogeneous boundary condition of the first kind at $z=0$ is

$$Z_n(z)=\sin(v_nz)$$

The homogeneous boundary condition of the second kind at $z=d$ yields the value of v_n, that is

$$v_n=(n-1/2)\pi/d \quad \text{for } n=1,2,3,\ldots$$

For homogeneous thermophysical properties in both layers, Eqs. (17a) and (17b) suggest that $\gamma=\eta$ and $\gamma_{np}=\gamma_p$. In addition, using Eq. (17a) one obtains

$$\beta_{np}=\sqrt{\gamma_p^2-v_n^2}$$

In the presence of contact resistance, the eigenvalues for the y-direction need to be computed numerically; however, when $R=0$, Eqs. (36) and (37) are equally valid for this example. According to Eqs. (36) and (37), there are two sets of eigenvalues that contribute to this solution. The examination of Eq. (32) reveals that, for the eigenvalues given by Eq. (37), the constant A_{np} vanishes when $p>1$ and $c-b=b$. Therefore, the temperature solution in this example is similar to Example 1 with A_{np} computed using equation

$$A_{np}=\frac{1}{N_{y,p}N_{z,n}}\frac{-q_0}{\beta_{np}\cosh(\beta_{np}a)}\int_{z=0}^{d}\sin[(n-1/2)\pi z/d]\,dz \times\left[\int_{y=0}^{b}\cos(\gamma_p y)\,dy+\int_{y=b}^{c}\{\overline{C}_p\cos[\lambda_{np}(y-b)] +\overline{D}_p\sin[\gamma_p(y-b)]\}\,dy\right] \quad (59)$$

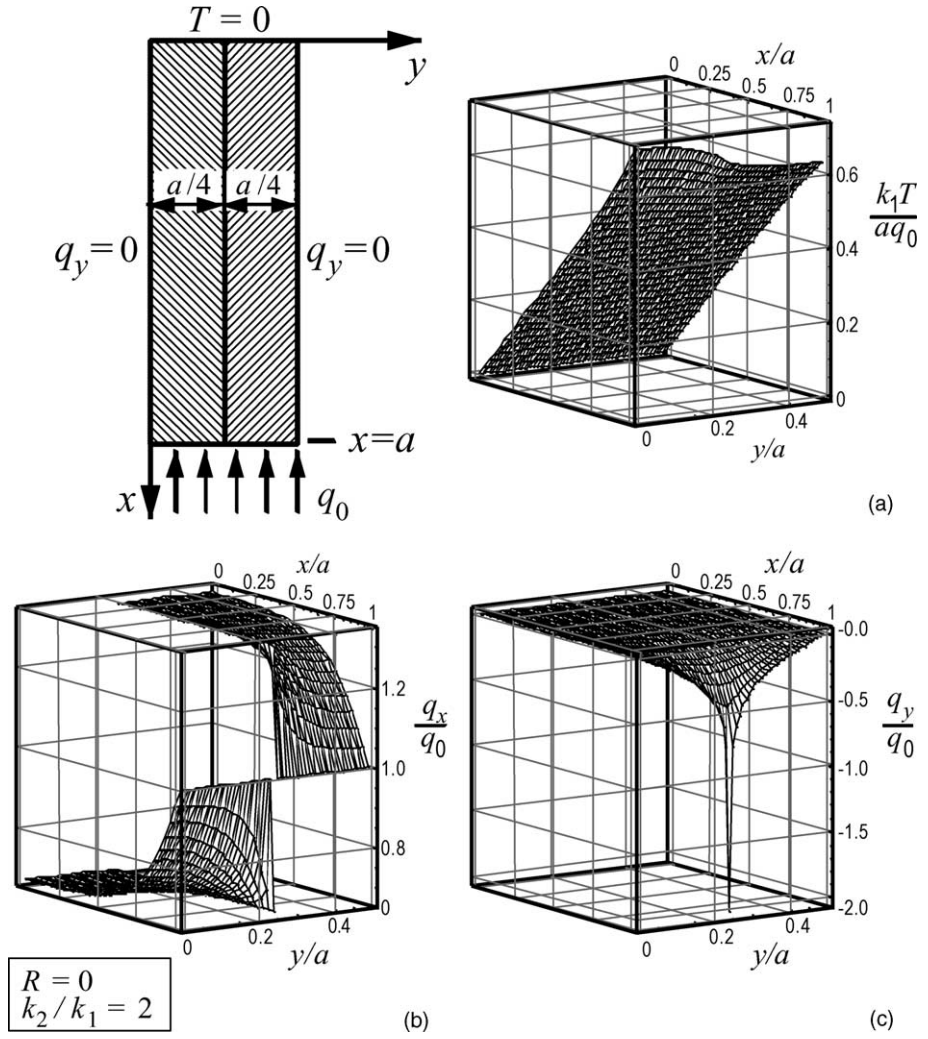

Fig. 3. Three-dimensional views of dimensionless (a) temperature $k_1T(x,y)/(aq_0)$, (b) x-component of heat flux vector q_x/q_0, and (c) y-component of heat flux vector q_y/q_0 as functions of x and y when $b/a = 1/4$.

wherein

$$\int_{z=0}^{d} \sin[(n-1/2)\pi z/d]\,\mathrm{d}z = \frac{-\cos[(n-1/2)\pi z/d]}{(n-1/2)\pi/d}\bigg|_{z=0}^{d} = \frac{d}{(n-1/2)\pi} \tag{60}$$

and $N_{z,n} = d/2$. After appropriate substitutions, the solutions in layers 1 and 2 for this highly simplified case are

$$T_1(x,y,z) = \frac{4q_0b}{k_1+k_2}\sum_{n=1}^{\infty}\frac{\sin[(n-1/2)\pi z/d]}{(n-1/2)\pi}\left\{\frac{d}{b(n-1/2)\pi} \times\left(\frac{\sinh[(n-1/2)\pi x/d]}{\cosh[(n-1/2)\pi a/d]}\right)-\left(\frac{k_2}{k_1}-1\right) \times\sum_{p=1}^{\infty}\left[\frac{(-1)^p\cos(\overline{\gamma}_p y/b)}{\overline{\gamma}_p\overline{\beta}_{np}}\left(\frac{\sinh(\overline{\beta}_{np}x/b}{\cosh(\overline{\beta}_{np}a/b)}\right)\right]\right\} \tag{61a}$$

$$T_2(x,y,z) = \frac{4q_0b}{k_1+k_2}\sum_{n=1}^{\infty}\frac{\sin[(n-1/2)\pi z/d]}{(n-1/2)\pi}\left\{\frac{d}{b(n-1/2)\pi} \times\left(\frac{\sinh[(n-1/2)\pi x/d]}{\cosh[(n-1/2)\pi a/d]}\right)-\left(\frac{k_2}{k_1}-1\right) \times\sum_{p=1}^{\infty}\left[\frac{k_1\sin(\overline{\gamma}_p(y-b)/b)}{k_2\overline{\gamma}_p\overline{\beta}_{np}}\left(\frac{\sinh(\overline{\beta}_{np}x/b}{\cosh(\overline{\beta}_{np}a/b)}\right)\right]\right\} \tag{61b}$$

where $\overline{\beta}_{np} = \beta_{np}b$.

To include the effect of contact resistance between the layers, the numerical computation of eigenvalues becomes necessary. After selecting the appropriate eigencondition from Table 3, the parameters γ and η were replaced by β using Eqs. (7a) and (7b). Then, the location of each eigenvalue was determined systematically by examining the right side and left side asymptotes of the

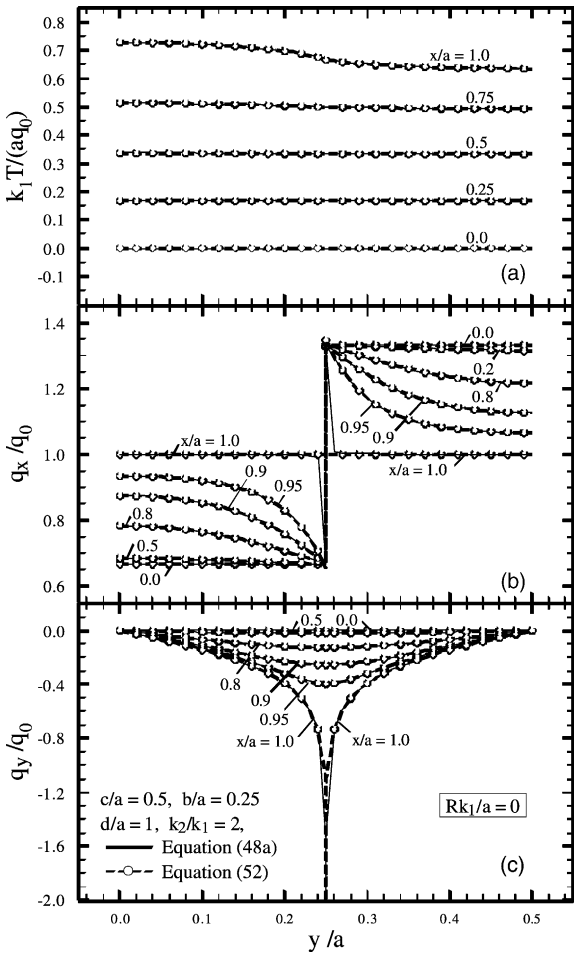

Fig. 4. (a) Dimensionless temperature $k_1T(x,y)/(aq_0)$, (b) x-component dimensionless heat flux q_x/q_0, and (c) y-component dimensionless heat flux q_y/q_0 as functions of y at different x/a values in Example 1.

eigencondition entry in Table 3. Each eigenvalue is located between two adjacent asymptotes. When there is no open space between two adjacent asymptotes, that location is where the eigenvalue is located [6]. Because each layer is homogeneous, all computed eigenvalues are real. As an illustration, following the computation of eigenvalues, temperature and heat flux components were computed and the results are in the forthcoming paragraph. A sophisticated numerical procedure [6] is used to acquire a large number of eigenvalues for the y-direction whenever necessary.

As in Example 1, there is an apparent singularity along the interface. Therefore, the following numerical studies address the variation of temperature and heat flux along the interface for layers 1 and 2. The solid lines in Fig. 5a describe the dimensionless interface temperature in layer 1 and the dash lines represent those in layer 2, both at $y = b$. For selected values of x, the data describe the variation of the temperature $k_1T(x,y)/(aq_0)$ as a function of the z/a. As expected from the compatibility conditions, in the absence of contact resistance, the difference between solid lines and dash lines is undetectable. Fig. 5b is prepared similar to Fig. 5a except there is a contact resistance $R_b = Rk_1/a = 0.1$ between the layers. The data show that the temperature difference across the contact zone gradually diminishes when $x/a < 0.6$. Next, all three components of the heat flux components are also computed and compared. Fig. 6a shows q_x/q_0 at the interface plotted versus z/a. Note that the data designated by dash lines in Fig. 6a are larger than the solid lines by a factor of $k_2/k_1 = 2$ while this difference is significantly reduced when there is contact resistance, see Fig. 6b. The effect of the singularity when $x/a = 1$ is evinced in Fig. 6a; however, it diminishes in the presence of contact resistance in Fig. 6b. In fact, in the presence of contact resistance, the heat flux data in Fig. 6b, are relatively well behaved along the $x = a$ plane. For a perfect contact condition, the heat flux data in the y-direction q_y/q_0 are in Fig. 7a. Similar data but in the presence of contact resistance are in Fig. 7b. Both sets of data satisfy the compatibility of heat flux at the interface as they indicate no difference across the contacting surfaces. The data plotted in Fig. 7a show a rapid reduction in heat flux near the heated surface as x/a decreases whereas in the presence of contact resistance, Fig. 7b, a gradual reduction of heat flux is detectable. A comparison of heat flux data, q_z/q_0, in Fig. 8a when $R_b = 0$ with those for $R_b = 0.1$ in Fig. 8b indicates that

Table 4
A comparison of convergence for two different solutions at $x/a = 1$

x/a	y/a	N-terms	Example 1, Eq. (48a)	Alternative solution, Eq. (52)
1.0	0.0	10	7.288656763773E−01	7.285378619630E−01
1.0	0.0	50	7.285508343313E−01	7.285373409979E−01
1.0	0.0	100	7.285339646374E−01	7.285373409979E−01
1.0	0.0	500	7.285358645438E−01	7.285373409979E−01
1.0	0.0	1000	7.285356980291E−01	7.285373409979E−01
1.0	0.0	2000	7.285357496316E−01	7.285373409979E−01

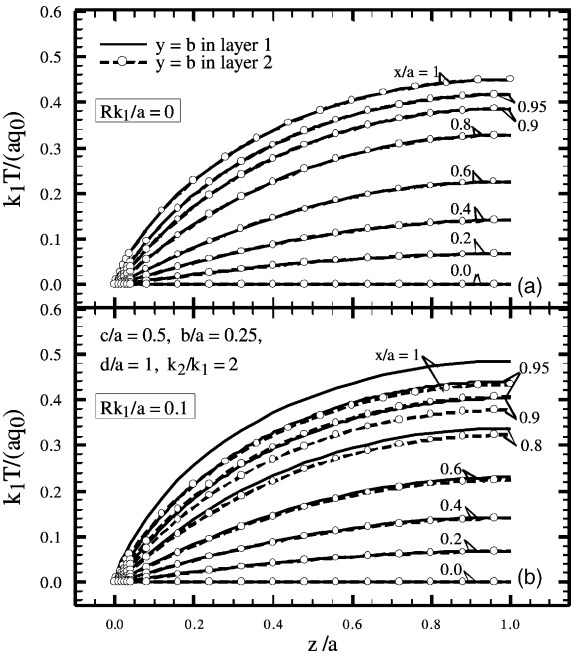

Fig. 5. A comparison of dimensionless temperature $k_1T(x,y)/(aq_0)$ at the interface for selected values of x/a: (a) when $R_b = 0$ and (b) when $R_b = 0.1$.

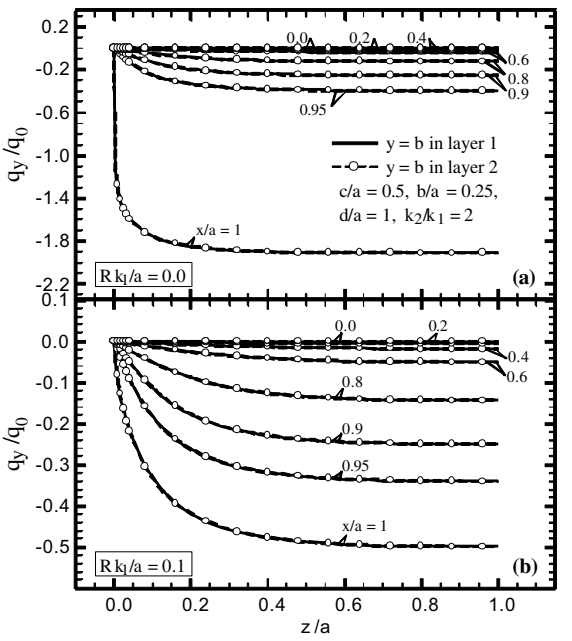

Fig. 7. A comparison of dimensionless heat flux q_y/q_0 at the interface for selected values of x/a: (a) when $R_b = 0$ and (b) when $R_b = 0.1$.

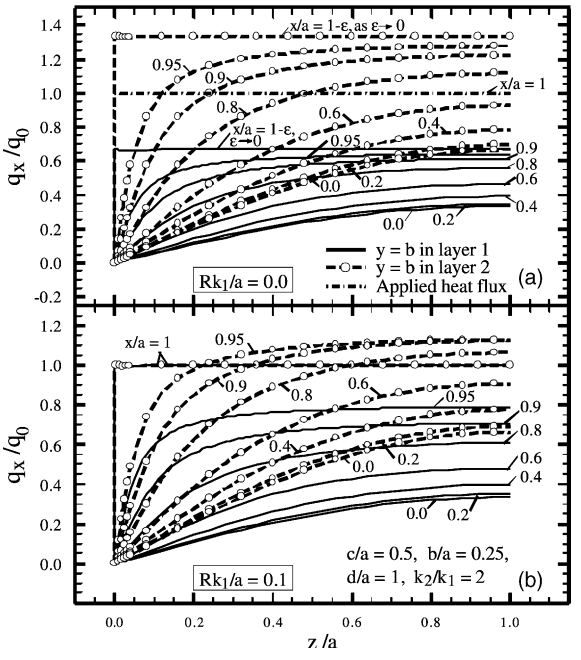

Fig. 6. A comparison of dimensionless heat flux q_x/q_0 at the interface for selected values of x/a: (a) when $R_b = 0$ and (b) when $R_b = 0.1$.

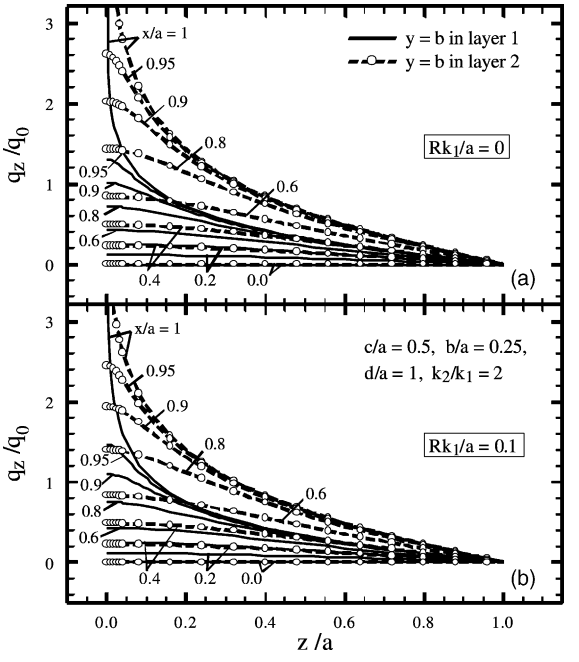

Fig. 8. A comparison of dimensionless heat flux q_z/q_0 at the interface for selected values of x/a: (a) when $R_b = 0$ and (b) when $R_b = 0.1$.

the effect of contact resistance is small. A small difference is detectable for large x/a values near $z = 0$ and, as expected, both Fig. 8a and b show relatively high heat flux values in the neighborhood of $z = 0$.

4. Remarks

The superposition of solutions, each having one nonhomogeneous boundary condition, is the viable method of solution. For example, when the solid depicted in Fig. 1 has insulating walls at $y = 0$, $y = c$, $x = 0$, and $x = a$ while the surface at $z = 0$ is kept at temperature $T_1 = T_2 = 0$ and there is a prescribed heat flux over $z = d$, the solution is as given in Example 1 but with some modifications. Eqs. (26a) and (26b), in Region 1 or 2, after appropriate modifications, become

$$T_1(x,y,z) = \sum_{p=1}^{\infty}\sum_{m=0}^{\infty} A_{mp}\sinh(v_{mp}z)\cos(m\pi x/a) \times \cos(\gamma_{mp}y) \tag{62a}$$

$$T_2(x,y,z) = \sum_{p=1}^{\infty}\sum_{m=1}^{\infty} A_{mp}\sinh(v_{mp}z)\cos(m\pi x/a) \times [\overline{C}_{mp}\cos[\eta_{mp}(y-b)] + \overline{D}_{mp}\sin[\eta_{mp}(y-b)] \tag{62b}$$

The remaining steps are identical to the case described in Example 1. One can compute temperature using Eqs. (45) and (46) after replacing x with z and a with d. When heat flux is prescribed over these two surfaces, the temperature solution is the sum of these two solutions. This superposition of solutions may be repeated for other nonhomogeneous conditions.

A steady-state solution can produce accurate temperature data in a layered material, except at the location where boundary conditions are nonhomogeneous. For an isotropic body, it is a simple task to provide a remedy for this deficiency. One can define a function T^* that can satisfy the nonhomogeneous boundary condition at that specific surface whose temperature is sought and use the relation

$$T = T^* + \theta$$

where θ would be the transformed temperature solution. This makes the boundary, whose temperature is needed, become homogeneous by altering other conditions. In many applications, this is a viable method of improving data accuracy for layered materials at the nonhomogeneous boundaries with uniform conditions of the first and third kind (constant temperature). However, because of the interface condition, the boundary conditions of the second kind are more demanding, as illustrated in Example 1.

The mathematical formulations presented in this paper are equally valid for layers with orthotropic thermal conductivities. The numerical computation of eigenfunctions may become demanding if the eigenvalues are imaginary. In this case, a methodology described in Ref. [4] may be used.

5. Conclusion

An accurate steady-state solution of a temperature field in a multi-layer body is an invaluable tool for analyzing heat spreaders in electronic cooling applications. This includes heat spreaders with orthotropic or isotropic layers. It can serve as an invaluable tool in analyzing thermal stress in various electronic devices.

An exact steady-state simulation can produce a high degree of accuracy away from the boundary with a nonhomogeneous boundary condition. In a three-dimensional study of transient problems, often a steady-state solution can reduce the computation time substantially by transferring the nonhomogeneous boundary conditions from the transient solution to a steady-state solution.

Acknowledgements

The work of first and second authors was supported in part by Sandia National Laboratories of Albuquerque, NM.

Appendix A. Orthogonality condition

It is necessary to establish an orthogonality condition for a specific case when there is a nonhomogeneous boundary condition over, e.g., the $x = a$ surface. A similar and parallel analysis applies to the case when the nonhomogeneous boundary condition is located over the $z = d$ surface. For simplicity of analysis, Eqs. (1a) and (1b) can be written as

$$\frac{\partial}{\partial x}\left[k_x(y)\frac{\partial T}{\partial x}\right] + \frac{\partial}{\partial y}\left[k_y(y)\frac{\partial T}{\partial y}\right] + \frac{\partial}{\partial z}\left[k_z(y)\frac{\partial T}{\partial z}\right] = 0 \tag{A.1}$$

It is assumed that the materials are orthotropic, Fig. 1, and the thermal conductivity values are independent of x and z but they change with y from layer to layer. For a series solution, the following relation describes the temperature,

$$T(x,y,z) = \sum_{m=1}^{\infty} X_m(x)\Psi_m(y,z) \tag{A.2}$$

Accordingly, each member $X_m(x)\Psi_m(y,z)$ of the set of solution functions must satisfy Eq. (A.1). For two specific

members $X_m(x)\Psi_m(y,z)$ and $X_n(x)\Psi_n(y,z)$, while assuming $X_m''(x)/X_m(x) = \beta_m^2$ and $X_n''(x)/X_n(x) = \beta_n^2$, Eq. (A.1) can be written as

$$-\beta_m^2 k_x(y)\Psi_m(y,z) = \frac{\partial}{\partial y}\left[k_y(y)\frac{\partial \Psi_m(y,z)}{\partial y}\right] + k_z(y)\frac{\partial^2 \Psi_m(y,z)}{\partial z^2} \tag{A.3}$$

and

$$-\beta_n^2 k_x(y)\Psi_n(y,z) = \frac{\partial}{\partial y}\left[k_y(y)\frac{\partial \Psi_n(y,z)}{\partial y}\right] + k_z(y)\frac{\partial^2 \Psi_n(y,z)}{\partial z^2} \tag{A.4}$$

Multiplying Eq. (A.3) by $\Psi_n(y,z)$ and Eq. (A.4) by $\Psi_m(y,z)$, and then subtracting the resulting equations following integration of both sides over y from 0 to c and over z from 0 to d yields the relation

$$\begin{aligned}
&\int_{z=0}^{d}\int_{y=0}^{c}(\beta_n^2-\beta_m^2)k_x(y)\Psi_m(y,z)\Psi_n(y,z)\,\mathrm{d}y\,\mathrm{d}z \\
&= \int_{z=0}^{d}\int_{y=0}^{c}\frac{\partial}{\partial y}\left\{\Psi_n(y,z)\left[k_y(y)\frac{\partial \Psi_m(y,z)}{\partial y}\right] - \Psi_m(y,z)\left[k_y(y)\frac{\partial \Psi_n(y,z)}{\partial y}\right]\right\}\mathrm{d}y\,\mathrm{d}z \\
&\quad + \int_{y=0}^{c}\int_{z=0}^{d}k_z(y)\frac{\partial}{\partial z}\left[\Psi_n(y,z)\frac{\partial \Psi_m(y,z)}{\partial z} - \Psi_m(y,z)\frac{\partial \Psi_n(y,z)}{\partial z}\right]
\end{aligned} \tag{A.5}$$

Both integrals on the right side of Eq. (A.5) vanish for boundary conditions specified in the text. This equation is equally valid in the presence of a temperature discontinuity at $y = b$ that makes $\Psi_n(y,z)$ also discontinuous. The term inside the curly brackets in Eq. (A.5) is continuous and it has a single value at the interface where $y = b$ for both layers. For layer 1, using the compatibility conditions, Eq. (9a), one can write the following term in Eq. (A.5) as

$$\begin{aligned}
&\left\{\Psi_n(y,z)\left[k_y(y)\frac{\partial \Psi_m(y,z)}{\partial y}\right] - \Psi_m(y,z)\left[k_y(y)\frac{\partial \Psi_n(y,z)}{\partial y}\right]\right\}_{\text{layer 1},y=b} \\
&= \Psi_{1,n}(b,z)[\Psi_{2,m}(b,z)-\Psi_{1,m}(b,z)]/R - \Psi_{1,m}(b,z) \\
&\quad \times [\Psi_{2,n}(b,z)-\Psi_{1,n}(b,z)]/R \\
&= [\Psi_{1,n}(b,z)\Psi_{2,m}(b,z) - \Psi_{1,m}(b,z)\Psi_{2,n}(b,z)]/R
\end{aligned}$$

Here, the subscripts 1 and 2 stand for layers 1 and 2 and R is the contact resistance. This process can be repeated for the same term at layer 2 using Eq. (9b) (or Eq. (9a)) to get

$$\begin{aligned}
&\left\{\Psi_n(y,z)\left[k_y(y)\frac{\partial \Psi_m(y,z)}{\partial y}\right] - \Psi_m(y,z)\left[k_y(y)\frac{\partial \Psi_n(y,z)}{\partial y}\right]\right\}_{\text{layer 2},y=b} \\
&= \Psi_{2,n}(b,z)[\Psi_{2,m}(b,z)-\Psi_{1,m}(b,z)]/R - \Psi_{2,m}(b,z) \\
&\quad \times [\Psi_{2,n}(b,z)-\Psi_{1,n}(b,z)]/R \\
&= [-\Psi_{2,n}(b,z)\Psi_{1,m}(b,z) + \Psi_{2,m}(b,z)\Psi_{1,n}(b,z)]/R
\end{aligned}$$

Since these two value are the same at $y = b$ (at the interface) for both layers; therefore, the term inside the curly brackets is continuous in the presence of a contact resistance. Finally, the orthogonality relation becomes,

$$(\beta_n^2-\beta_m^2)\int_{z=0}^{d}\int_{y=0}^{c}k_x(y)\Psi_m(y,z)\Psi_n(y,z)\,\mathrm{d}y\,\mathrm{d}z = 0 \tag{A.6}$$

and when $\beta_n \neq \beta_m$, then

$$\int_{z=0}^{d}\int_{y=0}^{c}k_x(y)\Psi_m(y,z)\Psi_n(y,z)\,\mathrm{d}y\,\mathrm{d}z = 0 \tag{A.7}$$

that can be written as

$$\int_{z=0}^{d}\left[\int_{y=0}^{b}k_{1x}\Psi_{1,m}(y,z)\Psi_{1,n}(y,z)\,\mathrm{d}y + \int_{y=b}^{c}k_{2x}\Psi_{2,m}(y,z)\Psi_{2,n}(y,z)\,\mathrm{d}y\right]\mathrm{d}z = 0 \tag{A.8}$$

This orthogonality relation includes the thermal conductivities in layers 1 and 2 as the weighting function. These derivations after minor modifications can be repeated when the nonhomogeneous boundary condition is along the z-direction.

References

[1] R.L. McMasters, Z. Zhou, K.J. Dowding, C. Somerton, J.V. Beck, Exact solution for nonlinear thermal diffusion and its use for verification, J. Thermophys. Heat Transfer 16 (2002) 366–372.

[2] R.L. McMasters, K.J. Dowding, J.V. Beck, D.H.Y. Yen, Methodology to generate accurate solutions for verification in transient three-dimensional heat conduction, Numer. Heat Transfer, Part B 41 (2002) 521–541.

[3] D.P. Kennedy, Spreading resistance in cylinderical semiconductor devices, J. Appl. Phys. 31 (1960) 1490–1497.

[4] S. Lee, S. Song, V. Au, K.P. Moran, Constriction/spreading resistance model for electronic packaging, in: Proceedings of the 4th ASME/JSME Thermal Engineering Joint Conference, vol. 4, 1995, pp. 199–206.

[5] M.M. Yovanovich, C.H. Tien, G.E. Schneider, General solution of constriction resistance within a compound disk, Heat Transfer, Thermal Control and Heat Pipes, AIAA Progress in Astronautics and Aeronautics, vol. 70, 1980.

[6] A. Haji-Sheikh, J.V. Beck, Temperature solution in multi-dimensional multi-layer bodies, Int. J. Heat Mass Transfer 45 (9) (2002) 1865–1877.
[7] C.W. Tittle, Boundary value problems in composite media, J. Appl. Phys. 36 (1965) 1486–1488.
[8] M.N. Ozisik, Heat Conduction, second edition, Wiley, New York, 1993.
[9] J.V. Beck, K. Cole, A. Haji-Sheikh, B. Litkouhi, Heat Conduction Using Green's Functions, Hemisphere Publ. Corp., Washington DC, 1992.
[10] K.J. Dowding, J.V. Beck, B.F. Blackwell, Estimation of directional-dependent thermal properties in a carbon–carbon composite, Int. J. Heat Mass Transfer 39 (1996) 3157–3164.
[11] C. Aviles-Ramos, A. Haji-Sheikh, J.V. Beck, Exact solution of heat conduction in composites and application to inverse problems, ASME J. Heat Transfer 120 (1998) 592–599.
[12] A. Haji-Sheikh, J.V. Beck, An efficient method of computing eigenvalues in heat conduction, Numer. Heat Transfer, B 38 (2000) 133–156.
[13] K.D. Cole, D.H.Y. Yen, Green's functions, temperature and heat flux in a rectangle, Int. J. Heat Mass Transfer 44 (2001) 3883–3894.
[14] D.H.Y. Yen, J.V. Beck, R.L. McMasters, D.E. Amos, Solution of an initial-boundary value problem for heat conduction in a parallelepiped by time partitioning, Int. J. Heat Mass Transfer 45 (2002) 4267–4279.